Virologica Sinica 38 (2023) 335–343

Contents lists available at ScienceDirect

Virologica Sinica

journal homepage: www.keaipublishing.com/en/journals/virologica-sinica
www.virosin.org

Research Article

Antibiotic-induced gut bacteria depletion has no effect on HBV replication in HBV immune tolerance mouse model

Yanan Bu [a], Kaitao Zhao [a], Zaichao Xu [a], Yingcheng Zheng [a], Rong Hua [a], Chuanjian Wu [a], Chengliang Zhu [b], Yuchen Xia [a,*], Xiaoming Cheng [c,*]

[a] State Key Laboratory of Virology and Hubei Province Key Laboratory of Allergy and Immunology, Hubei Jiangxia Laboratory, Institute of Medical Virology, TaiKang Center for Life and Medical Sciences, TaiKang Medical School, Wuhan University, Wuhan, 430071, China
[b] Department of Clinical Laboratory, Renmin Hospital of Wuhan University, Wuhan, 430060, China
[c] Department of Pathology, Center for Pathology and Molecular Diagnostics, Hubei Clinical Center and Key Laboratory of Intestinal and Colorectal Diseases, Zhongnan Hospital of Wuhan University, TaiKang Medical School, Wuhan University, Wuhan, 430071, China

ARTICLE INFO

Keywords:
Hepatitis B virus (HBV)
Gut bacteria
Antibiotic mixtures (ABX)
Adeno-associated virus (AAV)-HBV mouse model
Persistent HBV replication
Chronic HBV infection

ABSTRACT

Commensal microbiota is closely related to Hepatitis B virus (HBV) infection. Gut bacteria maturation accelerates HBV immune clearance in hydrodynamic injection (HDI) HBV mouse model. However, the effect of gut bacteria on HBV replication in recombinant adeno-associated virus (AAV)-HBV mouse model with immune tolerance remains obscure. We aim to investigate its role on HBV replication in AAV-HBV mouse model. C57BL/6 mice were administrated with broad-spectrum antibiotic mixtures (ABX) to deplete gut bacteria and intravenously injected with AAV-HBV to establish persistent HBV replication. Gut microbiota community was analyzed by fecal qPCR assay and 16S ribosomal RNA (rRNA) gene sequencing. HBV replication markers in blood and liver were determined by ELISA, qPCR assay and Western blot at indicated time points. Immune response in AAV-HBV mouse model was activated through HDI of HBV plasmid or poly(I:C) and then detected by quantifying the percentage of IFN-γ^+/CD8$^+$ T cells in the spleen *via* flow cytometry as well as the splenic IFN-γ mRNA level *via* qPCR assay. We found that antibiotic exposure remarkably decreased gut bacteria abundance and diversity. Antibiotic treatment failed to alter the levels of serological HBV antigens, intrahepatic HBV RNA transcripts and HBc protein in AAV-HBV mouse model, but contributed to HBsAg increase after breaking of immune tolerance. Overall, our data uncovered that antibiotic-induced gut bacteria depletion has no effect on HBV replication in immune tolerant AAV-HBV mouse model, providing new thoughts for elucidating the correlation between gut bacteria dysbiosis by antibiotic abuse and clinical chronic HBV infection.

1. Introduction

Hepatitis B virus (HBV) infection can lead to hepatitis, liver cirrhosis and even hepatocellular carcinoma. Approximate 300 million people are chronically infected with HBV worldwide, which heavily threatens global public health (Lee and Banini, 2019). HBV particles enter human hepatocytes *via* initial interaction with heparan sulfate proteoglycans (Xia et al., 2017) and subsequent binding between large envelope protein and sodium-taurocholate co-transporting polypeptide (Yan et al., 2012). After uncoating and capsid disassembly, HBV genome relaxed circular DNA (rcDNA) is released into nucleus, where rcDNA is converted into covalently closed circular DNA (cccDNA). HBV cccDNA can persist in the form of stable mini-chromosome and serve as the template for viral RNA transcription. Pregenomic RNA (pgRNA) together with viral polymerase is encapsulated into the new capsid and reversely transcribed into progeny rcDNA. Mature nucleocapsids either are enveloped *via* multivesicular body pathway for virion secretion or redirected to the nucleus to replenish cccDNA pool. Despite effectively suppressing virus loads, current approved therapies fail to eradicate HBV infection. In addition, many new therapeutic strategies such as capsid assembly modulators, entry inhibitors, RNA interference and therapeutic vaccines are still being under development (Xia and Liang, 2019).

Intestinal microbiota plays a fundamental role in maintaining host physical health. Gut microbiota dysbiosis is connected with manifold pathological processes including obesity, diabetes, carcinoma, gastrointestinal and neurological disorders (Durack and Lynch, 2019). Several strategies of manipulating gut microbes involving fecal microbiota transplantation (FMT), prebiotic diets and probiotic supplementation are

* Corresponding authors.
E-mail addresses: yuchenxia@whu.edu.cn (Y. Xia), xiaoming.cheng@whu.edu.cn (X. Cheng).

https://doi.org/10.1016/j.virs.2023.04.010
Received 29 January 2023; Accepted 26 April 2023
Available online 2 May 2023

being developed to overcome disorders, which provide promising therapeutic alternatives in recent decades (Wargo, 2020). The gut-liver axis is involved in the progression of chronic liver diseases. The liver secrets bile acids and immunoglobulin A into intestinal lumen *via* the biliary tract while host or gut microbial metabolites are transported into liver through the portal vein to modulate liver function (Almeida et al., 2022; Tripathi et al., 2018). The effect of gut microbiota alteration on HBV infection has been discovered in both mouse models and patients. In hepatitis B patients, gut microbiota richness and distribution were significantly different from those of healthy donors (Joo et al., 2021; Yang et al., 2020). Multiple FMT treatments significantly reduced hepatitis B e antigen (HBeAg) level by reshaping gut microbiota in HBeAg-positive patients after receiving long-term antiviral therapy (Ren et al., 2017). In HBV mouse models, Chou et al. uncovered the establishment of intestinal bacteria accelerated HBV immune clearance through Toll-like-receptor (TLR) 4 dependent pathway in C3H/HeN hydrodynamic injection (HDI) mouse model (Chou et al., 2015). Similarly, another two studies found gut bacteria depletion by antibiotics prolonged HBV infection through impairing liver T-cell antiviral immune response in C57BL/6 HDI mouse model (Guo et al., 2021; Wu et al., 2019). Besides, some evidence suggested that gut bacteria composition difference was responsible for HBV susceptibility in C57BL/6 and BALB/c mouse models mediated by HDI of HBV plasmid (Wang et al., 2022). These results collectively indicated antibiotic-induced gut bacteria alteration suppressed HBV immune clearance in HDI HBV mouse model. However, HDI mouse model is featured with activation of HBV-specific immune response and liver damage, making it not optimal to study the effect of gut bacteria on immune tolerant phase (Bertoletti and Ferrari, 2016). Therefore, investigations are necessary to shed light on the potential effect of gut bacteria on HBV immune tolerance mouse models.

AAV-HBV viral vector transduced mouse model can simulate chronic HBV carriers considering the advantages of HBV cccDNA formation (Lucifora et al., 2017; Xu et al., 2022), persistent HBV replication for more than one year and no obvious HBV immune response (Yang et al., 2014), which is suitable for dissecting host-virus interaction (Teng et al., 2021) and developing antiviral agents for chronic HBV infection (Xu et al., 2022). In this study, we injected recombinant AAV-HBV into mice to establish persistent HBV replication and supplemented antibiotic mixtures to deplete gut bacteria before or after the establishment of HBV replication. Our data revealed the great loss of gut microbiota community by antibiotic treatment. However, HBV replication levels remain unaffected in those AAV-HBV mice, regardless of gender. Our data suggest that gut bacteria depletion has minimal effect on HBV replication in HBV immune tolerance phase.

2. Materials and methods

2.1. Recombinant AAV-HBV production

The plasmind pAAV-HBV1.3 or pAAV-HBV1.2 was constructed by inserting 1.3 or 1.2-fold HBV genome, genotype D (GenBank accession number: V01460.1) into an AAV2 ITR containing plasmid (Lucifora et al., 2017). HEK293T cells were cultured in DMEM (Gibco, USA) with 10% FBS, 1% penicillin/streptomycin and maintained with 5% CO_2 at 37 °C. Plasmids (pAAV-HBV1.3 or pAAV-HBV1.2, pAAV2/8-RC and pHelper) were co-transfected into HEK293T cells in 1:1:1 M ratio using PEI MAX 40K (Polysciences, USA). The supernatant and cell pellets were harvested at 72 h post transfection, then filtered with 0.22 μm sterile filters and concentrated with Amicon Ultra-15 (Millipore, USA) centrifugal filter unit. Recombinant AAV-HBV titer was quantified by qPCR assay.

2.2. Animal experiments

C57BL/6 mice (female and male, 5–6 weeks old) were purchased from China Three Gorges University Laboratory Animal Center (Yichang, China) and maintained in animal room at constant temperature (24 ± 2 °C) and humidity (55% ± 2%) with 12 h light/dark cycle. The mice acclimated to the environment for 3–4 days before all experiments were carried out. To establish AAV-HBV mouse model, recombinant virus (5×10^{10} viral genome AAV-HBV1.3 or 1×10^{11} viral genome AAV-HBV1.2 diluted into 200 μL PBS) were injected through tail vein. To establish HDI mouse model, 6 μg of pAAV-HBV1.2 plasmid was rapidly injected into mouse following previous procedures (Huang et al., 2006). Polyinosinic-polycytidylic acid [poly(I:C)] was dissolved in sterilized water and saved in −80 °C (MCE, USA). After dilution into sterilized PBS buffer, 20 μg of poly(I:C) was rapidly injected into mice.

2.3. Antibiotic treatment

A well-established antibiotic mixture (ABX) protocol including 1 g/L metronidazole (Solarbio, China), 1 g/L neomycin sulfate (Solarbio, China), 0.5 g/L vancomycin (Biosharp, China) and 1 g/L ampicillin (Biofroxx, China) dissolved in sterile water was used to deplete gut microbiota. Drinking water with or without antibiotics was replenished every three days after sterilized with 0.22 μm filters.

2.4. Total RNA extraction and HBV RNA determination

The fresh liver tissues were snap-frozen and stored at −80 °C after taken from mouse body. Estimated 30 mg tissues were homogenized to extract total RNA using RNApure Tissue & Cell Kit (CWBIO, China). RNA quality was assessed using Nanodrop (ThermoFisher Scientific, USA) and then cDNA was prepared by ReverTra Ace qPCR RT Master Mix (TOYOBO, Japan) following the manufacturer's instructions. Relative RNA levels were determined by a LightCycler 480 system (Roche Diagnostics, Switzerland) and calculated by the calibrator-normalized Relative Quantification of the instrument operator's manual with mouse *Actb* as the reference gene. Primers were listed in Supplementary Table S1.

2.5. The detection of serological HBeAg and hepatitis B surface antigen (HBsAg)

Mouse blood samples were collected at different time points and then serum samples were obtained after centrifugation at 1000×*g* for 10 min. Serum samples were diluted with PBS to determine HBeAg and HBsAg by ELISA Kit (KHB, China) according to the manufacturer's instructions. Absorbance value at 450 nm was read by a microplate reader (HIDEX, Finland).

2.6. Western blot

Fresh mouse liver tissues were suspended in RIPA protein lysis buffer (Sigma-Aldrich, USA) with protease inhibitor cocktail and homogenized using Tissue Cell-Destroyer DS1000 (Novastar, China). After lysis for 30 min on ice, the supernatant was harvested *via* centrifugation at 4 °C, 12,000 ×*g* for 10 min. The protein concentration of liver tissues was determined using BCA Assay Kit (Biosharp, China). Equivalent protein samples were separated by SDS-PAGE and transferred into PVDF membranes (Millipore, USA). After blocked by 5% nonfat milk at room temperature for 1 h, the membranes were incubated with the primary antibody overnight at 4 °C followed by incubation with the secondary antibody. At last, all protein bands were shown using Immobilon Western Chemiluminescent HRP substrate (Millipore, USA) by a Luminescent Image Analyzer (Syngene, UK). Details of antibodies were listed in Supplementary Table S2.

2.7. Fecal DNA extraction and 16S rRNA gene determination by qPCR assay

To analyze the composition of gut bacteria, fresh fecal pellets were collected and total genome DNA was extracted using TIANamp Stool

DNA Kit (TIANGEN, China) according to the manufacturer's protocols. Genome DNA was quantified by Nanodrop (ThermoFisher Scientific, USA) and then diluted at 10 ng/μL for bacterial 16S rRNA gene qPCR assay. Specific 16S rRNA gene primers were listed in Supplementary Table S1.

2.8. Fecal 16S rRNA gene sequencing

Fresh mouse stool samples were collected from individual mouse and immediately stored at −80 °C until use. Total genome DNA was isolated using a TIANamp Stool DNA Kit (TIANGEN, China) following the manufacturer's instructions. The total bacterial 16S rRNA gene was amplified with primers targeting the V3–V4 (341 F and 805 R) region. PCR products were purified and normalized for sequencing using the Illumina Novaseq 6000 platform. Effective reads were obtained after primer removal, sequence splicing and length filter from raw data. Operational taxonomic units (OTUs) were identified under the level of 97% similarity using UPARSE. Taxonomic annotation of feature sequences was performed using Naive Bayes classifier according to SILVA database to count community composition at different levels. In brief, QIIME software (Bolyen et al., 2019) was used to analyze alpha diversity including Chao1 and Shannon index and beta diversity was mainly represented by Principal coordinate analysis (PCoA). Line Discriminant Analysis (LDA) Effect Size (LEfSe) was intended for statistically significant biomarkers between two groups.

2.9. Flow cytometry

Mouse spleens were extracted and homogenized in sterilized PBS buffer. The splenocytes were cultured in RPMI 1640 (Gibco, USA) with 10% FBS, 1% penicillin/streptomycin and stimulated with the $HBsAg_{190–197}$ (VWLSVIWM) peptide (QYAOBIO, China). After incubation with cell-surface antibodies, splenocytes were fixed, permeated and stained with intracellular antibodies. Data were collected using CytoFLEX S (BECKMAN-COULTER, USA) and analyzed *via* CytExpert software version 2.4 (BECKMAN-COULTER, USA). Details of antibodies were listed in Supplementary Table S2.

2.10. Statistical analysis

Statistical analysis was performed using GraphPad Prism 7.0 software (GraphPad Software, USA). The unpaired two-tailed Student's *t*-test was carried out to compare differences between two groups. The log rank test was adopted in Fig. 1E. Data were presented as the mean ± standard error of mean (SEM) and $P < 0.05$ was considered significant.

3. Results

3.1. Gut microbiota depletion by antibiotics hinders HBV immune clearance in male HDI mouse model

We first followed previous study procedures by using HDI mouse model (Wu et al., 2019). Five-week-old male C57BL/6 mice were orally administrated with a mixture of broad-spectrum antibiotics (Morgun et al., 2015; Zarrinpar et al., 2018) for 4 weeks and then received 6 μg pAAV-HBV1.2 plasmid through HDI (Fig. 1A). Mouse body weights were not changed (Fig. 1B) while gut bacteria richness was significantly reduced (Fig. 1C) during antibiotic exposure. HBV replication markers were assessed from 2 days post injection (dpi) to 6 weeks post injection (wpi). Compared to control group, the slightly higher serum HBeAg level

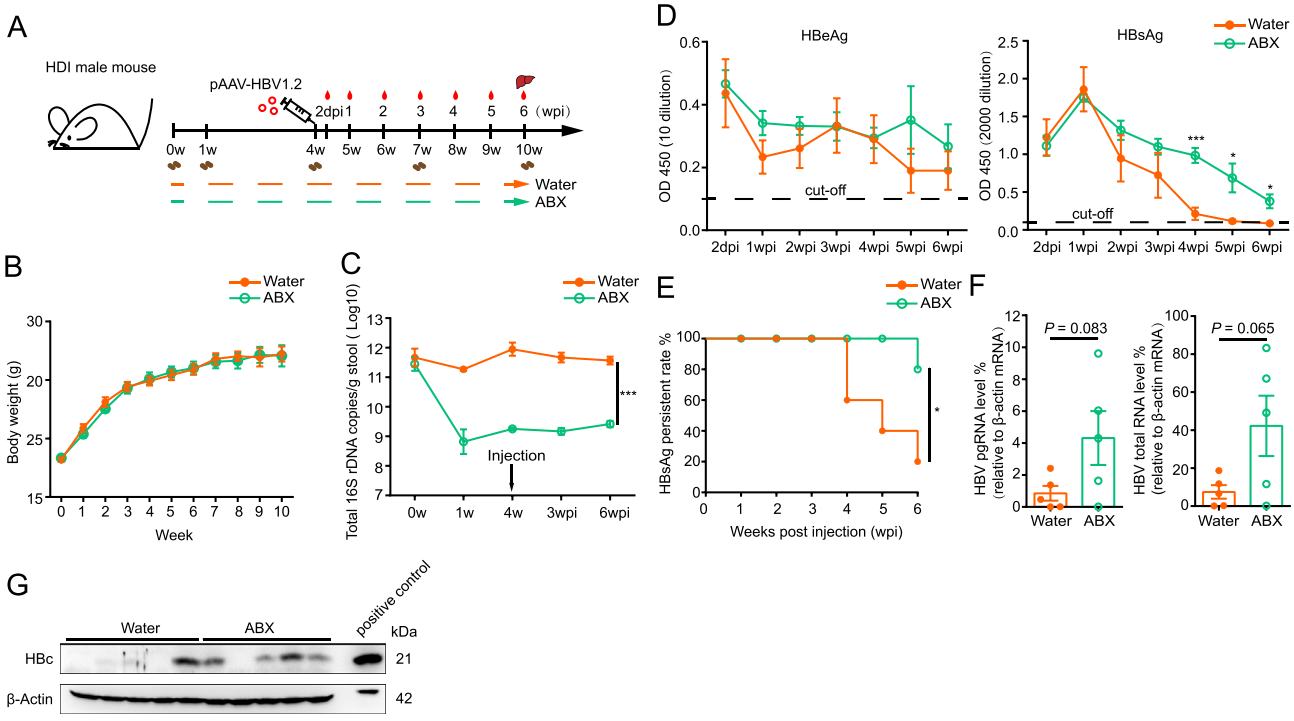

Fig. 1. The effect of antibiotic-induced gut microbiota depletion on HBV replication in male hydrodynamic injection (HDI) mouse model. **A** Five-week-old male mice were fed with water or water with antibiotic mixtures (ABX) for 4 weeks and were then hydrodynamically injected with 6 μg pAAV-HBV1.2 plasmid (water group: n = 5; ABX group: n = 5). **B** Body weights at indicated time points were shown. **C** The amount of total gut bacteria was determined by qPCR assay after collection of stool samples. **D** Mouse serum HBeAg and HBsAg level were detected by ELISA once a week from 2 dpi to 6 wpi (the cut-off value is 0.1, provided by the kit). **E** Serum HBsAg persistent rate (OD 450 > 0.1) was counted. **F** Mouse liver tissues were collected at 6wpi and RNA isolation and cDNA preparation were performed. Levels of intrahepatic HBV pgRNA ($P = 0.083$) and total RNA ($P = 0.065$) were assessed by qPCR assay with mouse *Actb* as the reference gene. The relative level was calculated by the calibrator-normalized Relative Quantification of LightCycler 480 instrument operator's manual. **G** The higher level of intrahepatic HBc protein expression caused by antibiotics was verified by Western blot at 6 wpi. HBV-expressing cell line HepAD38 was positive control in Western blot. Data are presented as mean ± standard error of mean. Statistical analysis was performed by Student's unpaired two-tailed *t*-test, $^{*}P < 0.05$, $^{***}P < 0.001$.

was maintained (Fig. 1D, left) in antibiotic-treated group. In addition, the decline of HBsAg level was strongly delayed by antibiotics from 4 wpi to 6 wpi (Fig. 1D, right), in which 80% (4 of 5) of antibiotic-treated mice still remained HBsAg positive up to 6 wpi (Fig. 1E). Besides, more viral transcripts including pgRNA and total RNA (Fig. 1F) were determined in ABX group. Hepatitis B core (HBc) protein expression was also increased in mouse liver tissues after antibiotic treatment (Fig. 1G). Next, we repeated this experiment and collected mouse spleen samples at different time points for HBV immune response determination (Supplementary Fig. S1A). Similar results were observed in serum HBsAg clearance (Supplementary Fig. S1B). Accordingly, IFN-γ mRNA expression in spleen of control group was higher than that of ABX group at 4 wpi, suggesting attenuated HBV immune response caused by antibiotic treatment (Supplementary Fig. S1C). In conclusion, consistent with previous studies, antibiotic-induced gut bacteria depletion prolonged HBV persistence and impeded HBV immune response in male HDI mouse model.

3.2. Intestinal bacteria depletion by antibiotics has no effect on HBV replication in established female AAV-HBV mouse model

Without activation of strong HBV immune response, AAV-HBV mouse model is superior to mimic clinical chronic HBV infection at immune tolerance phase (Yang et al., 2014). We previously established AAV-HBV mouse model through intravenously injecting recombinant adeno-associated virus carrying 1.3-fold length of HBV genome (AAV-HBV1.3) into six-week-old female C57BL/6 mice. Fecal pellets and blood samples were collected at indicated times points for studying gut bacteria composition and HBV replication outcomes, respectively. Mouse liver tissues were obtained after euthanasia at the time point of 14 and 38 weeks post antibiotic treatment (Fig. 2A). Persistent lower abundance of total gut bacteria was determined throughout antibiotic administration (Fig. 2B). In particular, amounts of *Escherichia coli* and *Klebsiella pneumoniae* of *Enterobacteriaceae* were increased while *Enterococcus* and *Lactobacillus* were decreased significantly in ABX group (Fig. 2C). Furthermore, gut microbiome was analyzed by fecal 16S rRNA gene sequencing. Antibiotics contributed to massive decrease of average operational taxonomic unit (OTU) counts, Shannon index and Chao1 index (alpha diversity) (Fig. 2D) and structural changes (beta diversity) (Fig. 2E) of commensal microbiota. At the genus level, gut microbiota profiles were obviously shifted in ABX group, with various bacteria decreased (*uncultured_bacterium_f_Muribaculaceae*, *Lactobacillus*, *Lachnospiraceae_NK4A136_group* and *Dubosiella*) and several predominant bacteria increased (*uncultured_bacterium_f_Enterobacteriaceae* and *Bacteroides*) (Fig. 2F, Supplementary Fig. S2A and S2B). In addition, antibiotics resulted in significant increase in caecum weight and size (Supplementary Fig. S2C and S2D). In a word, the

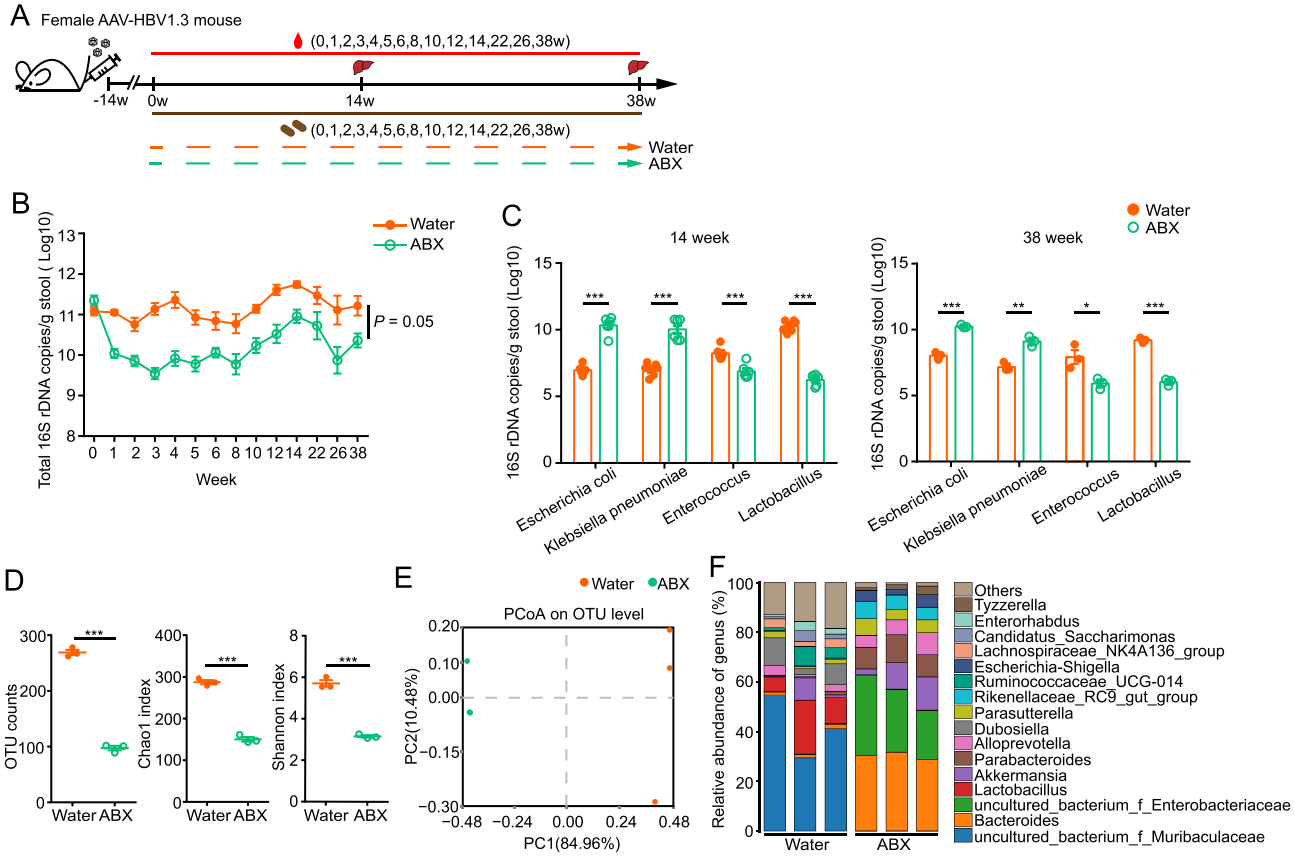

Fig. 2. The effect of 38-week antibiotic administration on gut bacteria in established female AAV-HBV1.3 mouse model. **A** Female AAV-HBV1.3 mice (n = 12, 5×10^{10} viral genome AAV-HBV1.3 was injected 14 week before antibiotic treatment) were randomly assigned into two groups respectively: one group was treated with antibiotics (ABX group, n = 6) and the other was not (water group, n = 6). **B** Total 16S rRNA gene copies of gut bacteria in fecal were quantified by qPCR assay. **C** The amounts of *Escherichia coli*, *Klebsiella pneumoniae*, *Enterococcus* and *Lactobacillus* in stool samples were determined by qPCR assay after 14-week and 38-week antibiotic treatment. **D** Operational taxonomic unit (OTU) counts, Chao1 index and Shannon index were assessed for alpha diversity. **E** Beta diversity was analyzed *via* principal coordinate analysis (PCoA) based on Bray-Curtis distance (ANOSIM R = 1, $P = 0.1$) of two groups. **F** Differential microbiota species distribution in fecal at the genus level among individual mouse. Data are presented as mean ± standard error of mean. Statistical analysis was performed by Student's unpaired two-tailed *t*-test, $^{*}P < 0.05$, $^{**}P < 0.01$, $^{***}P < 0.001$.

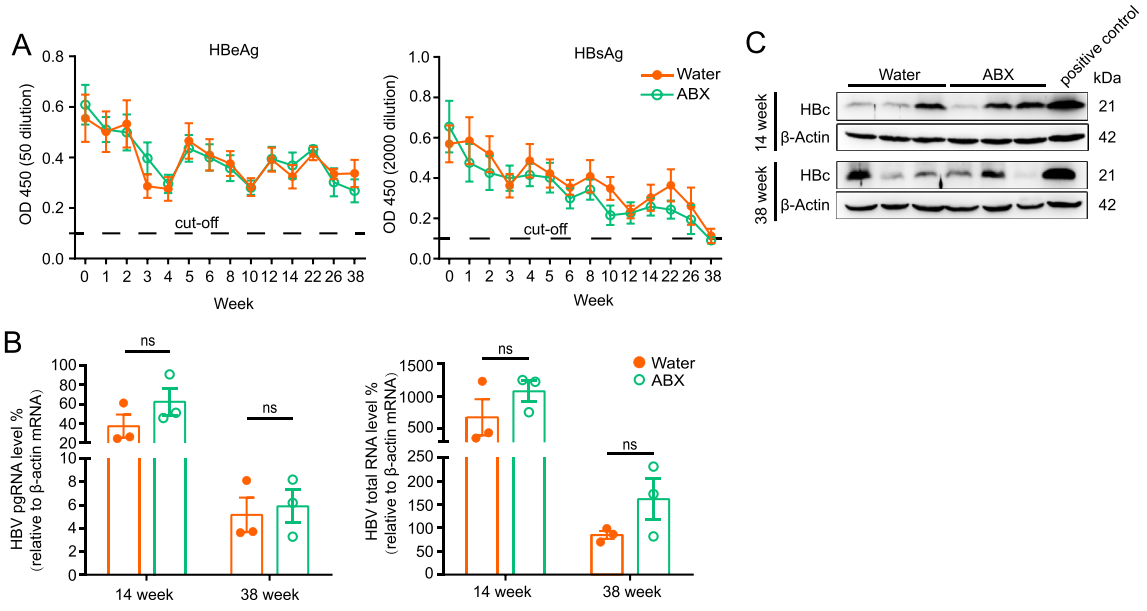

Fig. 3. The effects of 38-week antibiotic treatment on HBV replication in established female AAV-HBV1.3 mouse model. **A** Serum samples were diluted into PBS buffer and HBeAg and HBsAg levels were determined with ELISA during antibiotic intervention. Mouse liver tissues were collected after 14 and 38-week antibiotic treatment for RNA and protein extraction. Levels of HBV pgRNA and HBV total RNA (**B**) were evaluated by qPCR assay with mouse *Actb* as the reference gene. The relative level was calculated by the calibrator-normalized Relative Quantification of LightCycler 480 instrument operator's manual. HBc protein expression in liver was shown *via* Western blot (**C**). HBV-expressing cell line HepAD38 was positive control in Western blot. Data are presented as mean ± standard error of mean. Statistical analysis was performed by Student's unpaired two-tailed *t*-test, $^{*}P < 0.05$, $^{**}P < 0.01$, $^{***}P < 0.001$, ns: no significance.

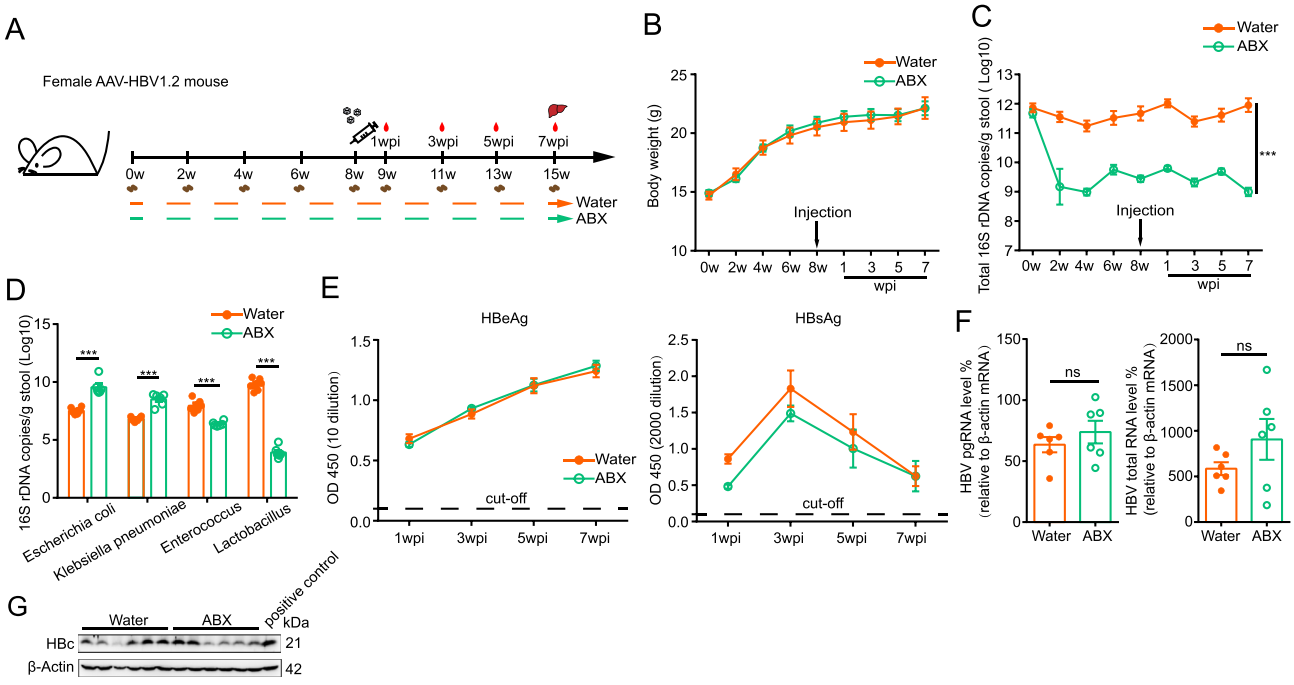

Fig. 4. The effect of antibiotic-induced gut microbiota depletion before injection on HBV replication in female AAV-HBV1.2 mouse model. **A** Five-week-old female mice were administrated with antibiotic mixtures (ABX) in drinking water for 8 weeks and were then injected with 1×10^{11} viral genome recombinant AAV-HBV1.2 *via* tail vein. The body weights were monitored (**B**) and stool samples were collected for total gut bacteria amount determination by qPCR assay (**C**) before and after injection. **D** Specific species of gut bacteria in stool samples including *Escherichia coli*, *Klebsiella pneumoniae*, *Enterococcus* and *Lactobacillus* were quantified by qPCR assay at 7 weeks post injection (wpi). **E** HBeAg and HBsAg levels in mouse serum were detected by ELISA at different time points (cut-off value = 0.1). **F** Intrahepatic HBV pgRNA and HBV total RNA levels were detected by qPCR assay after RNA isolation and reverse transcription, with mouse *Actb* as the reference gene. The relative level was calculated by the calibrator-normalized Relative Quantification of LightCycler 480 instrument operator's manual. **G** HBc protein in mouse liver tissues was displayed by Western blot at 7 wpi. HBV-expressing cell line HepAD38 was positive control in Western blot. Data are presented as mean ± standard error of mean. Statistical analysis was performed by Student's unpaired two-tailed *t*-test, $^{***}P < 0.001$, ns: no significance.

richness and diversity of gut microbiota were profoundly dropped by antibiotic treatment, which confirmed the antibiotic efficacy on gut bacteria depletion. However, serum HBeAg and HBsAg levels were not altered at each time point of antibiotic intervention (Fig. 3A). In addition, intrahepatic HBV replication markers including levels of HBV pgRNA, HBV total RNA (Fig. 3B) and HBc protein (Fig. 3C) remained unchanged after antibiotic treatment. These results indicated that intestinal bacteria depletion by antibiotics failed to affect HBV replication in established female AAV-HBV mouse model.

3.3. Commensal bacteria depletion by antibiotics before infection is unable to affect HBV replication in female AAV-HBV mouse model

Considering that gut bacteria dysbiosis by antibiotic abuse greatly enhanced the risk of pathogen infection (Croswell et al., 2009; Drummond et al., 2022; Erttmann et al., 2022), we planned to disrupt gut bacteria community before infection for evaluating HBV persistence in AAV-HBV mouse model. As shown in Fig. 4A, five-week-old female C57BL/6 mice received the antibiotic cocktails for 8 weeks and then recombinant adeno-associated virus carrying 1.2-fold length of HBV genome (AAV-HBV1.2) was delivered into mice through intravenous injection. The mouse serum HBV antigens were detected every 2 weeks. Liver tissues were collected for determination of intrahepatic HBV replication markers at 7 wpi. Compared with control group, mouse weight of ABX group showed no difference before and after AAV-HBV injection (Fig. 4B). Antibiotic treatment dramatically reduced total gut bacteria abundance at different time points (Fig. 4C) as well as altered specific microbe amounts (Fig. 4D). As for HBV replication outcomes, serum HBeAg and HBsAg levels of ABX group were similar to those of control group except the higher HBsAg level at 1 wpi in control group (Fig. 4E). In line with this, antibiotic administration failed to affect intrahepatic viral RNA transcription (Fig. 4F) and HBc protein expression (Fig. 4G). These data suggested that antibiotic exposure before infection was also unable to affect HBV replication in female AAV-HBV mouse model.

3.4. Antibiotic-induced gut bacteria disruption imposes no effect on HBV replication in male AAV-HBV mouse model

It has been noted that male mouse expresses higher levels of HBV antigens than female mouse (Yang et al., 2014; Kosinska et al., 2017). The effect of gut bacteria on HBV replication was investigated in male AAV-HBV mouse model in the following experiments. We established persistent HBV infection in male mouse *via* intravenous injection of recombinant AAV-HBV1.2 and then split mice into control group and ABX group (Fig. 5A). Mouse weight and total gut bacteria amount were monitored during the whole antibiotic treatment period. Antibiotic exposure had no effect on body weights (Fig. 5B) and led to the lower gut bacteria abundance (Fig. 5C). With regard to HBV replication levels, slightly higher serum HBeAg and HBsAg levels were observed in ABX group but displayed no significance in statistical analysis (Fig. 5D). Meanwhile, neither levels of intrahepatic HBV RNA transcripts (Fig. 5E) nor HBc protein (Fig. 5F) were affected by antibiotics. From these results, antibiotic exposure after HBV infection did not affect HBV replication in male AAV-HBV mouse model.

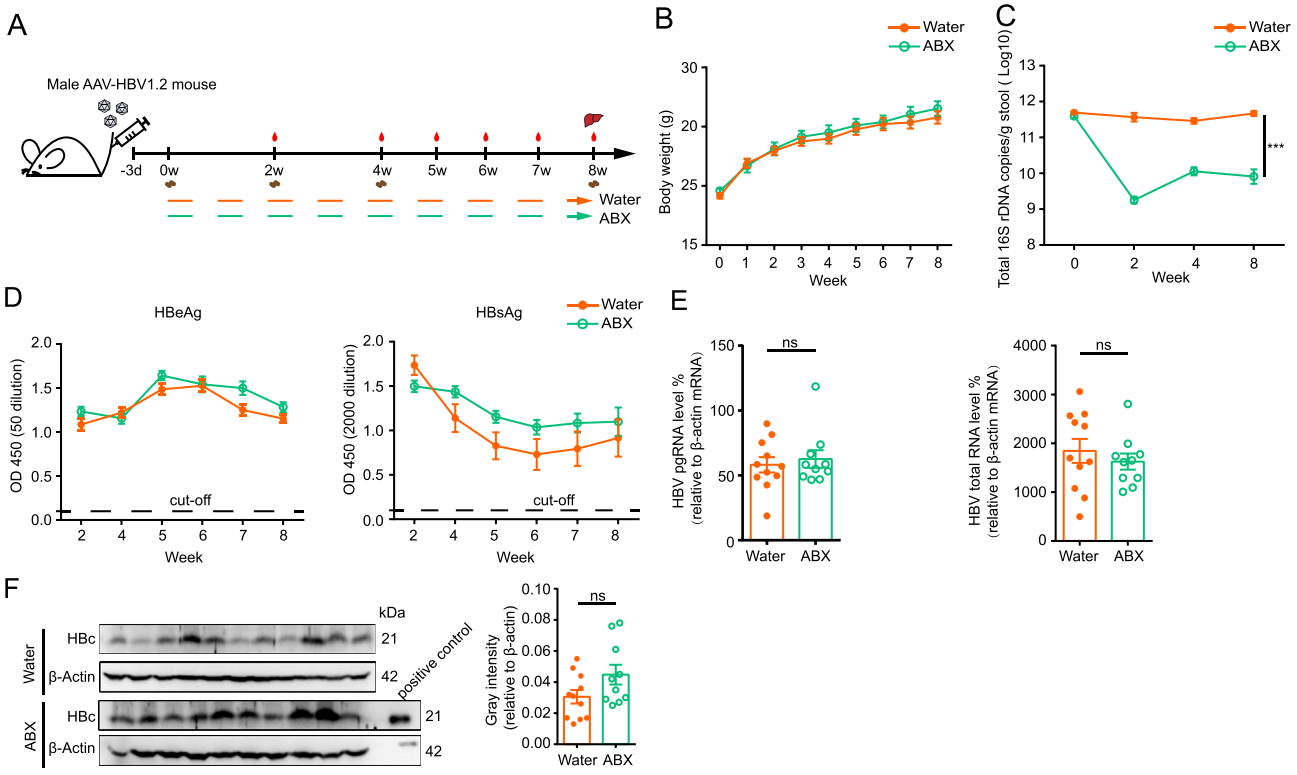

Fig. 5. The effect of antibiotic-induced gut microbiota depletion on HBV replication in male AAV-HBV1.2 mouse model. **A** Six-week-old male mice received 1×10^{11} viral genome recombinant AAV-HBV1.2 and were then split into water group (n = 11) and ABX group (n = 10). Mice in ABX group were fed with antibiotics for 8 weeks. **B** Body weights of all mice were recorded once a week. **C** Total gut bacteria amount of stool samples was quantified by qPCR assay during antibiotic administration. **D** The levels of serum HBeAg and HBsAg were detected using ELISA kit from 2 weeks to 8 weeks (cut-off value = 0.1). **E** Levels of intrahepatic HBV pgRNA and HBV total RNA were measured by qPCR assay after liver RNA extraction and cDNA preparation, with mouse *Actb* as the reference gene. The relative level was calculated by the calibrator-normalized Relative Quantification of LightCycler 480 instrument operator's manual. **F** HBc protein level at the experiment endpoint was shown by Western blot. Gray intensity analysis was performed *via* Image J to compare HBc protein level. HBV-expressing cell line HepAD38 was positive control in Western blot. Data are presented as mean ± standard error of mean. Statistical analysis was performed by Student's unpaired two-tailed *t*-test, $^{***}P < 0.001$, ns: no significance.

3.5. Antibiotic-induced gut bacteria alteration affects HBV replication after breaking of immune tolerance

Of note, HBV immune response can be detected in both transient and persistent HBV replication HDI mouse model (Huang et al., 2006; Wang et al., 2018), while AAV-HBV transduced mouse model is characterized as immune tolerance (Dion et al., 2013). Existing evidence has showed that antibiotic-induced gut bacteria depletion impairs HBV immune response, thus delaying HBV clearance in HDI mouse model (Wu et al., 2019). Here, we showed that antibiotic-caused gut bacteria depletion did not affect HBV replication in AAV-HBV transduced mouse model. Thus, we reasoned that antibiotic-induced gut bacteria depletion might affect HBV replication only when HBV immune response was stimulated. To address this issue, we established persistent HBV replication through injecting AAV-HBV1.2 into male C57BL/6 mouse model and then altered gut bacteria *via* antibiotic supplement into drinking water for 4 weeks, and then injected pAAV-HBV1.2 or poly(I:C) *via* HDI to break the immune tolerance (Fig. 6A). Consistent with our previous results, antibiotic treatment failed to affect HBV replication in AAV-HBV mouse model before pAAV-HBV1.2 or poly(I:C) HDI (Fig. 6B). As expected, both pAAV-HBV1.2 and poly(I:C) were able to significantly increase splenic HBV specific IFN-γ^+/CD8$^+$ T cells (Fig. 6C), which is consistence with splenic IFN-γ mRNA levels (Fig. 6D). These results indicated HBV immune response in male AAV-HBV1.2 mouse model was activated. Interestingly, in both pAAV-HBV1.2 and poly(I:C) stimulation groups, antibiotic exposure elevated serum HBsAg levels (Fig. 6E). In conclusion, our results demonstrated antibiotic-caused gut bacteria alteration increased HBV replication in male AAV-HBV mouse model after breaking immune tolerance.

4. Discussion

Increased evidence has demonstrated the association between gut bacteria dysbiosis and HBV-related liver diseases (Fox et al., 2010; Huang et al., 2020), and the elucidation about the role of gut bacteria at the stage of chronic HBV infection is still needed. In previous studies, researchers delivered broad-spectrum antibiotic cocktails to HDI HBV mouse model and uncovered intestinal microbe integrity prompted HBV immune clearance (Chou et al., 2015; Wu et al., 2019). However, when it comes to deficient HBV-specific immune response in chronic HBV patients, HBV immune tolerance mouse model is preferred to study the effect of gut bacteria on HBV replication (Du et al., 2021). Hence, AAV-HBV mouse model lacking immune response was utilized in our experiments.

Mice were treated with the same antibiotic mixtures to disrupt gut bacteria community. Fecal qPCR assay and 16S rRNA gene sequencing suggested that the abundance and diversity of gut microbiota were

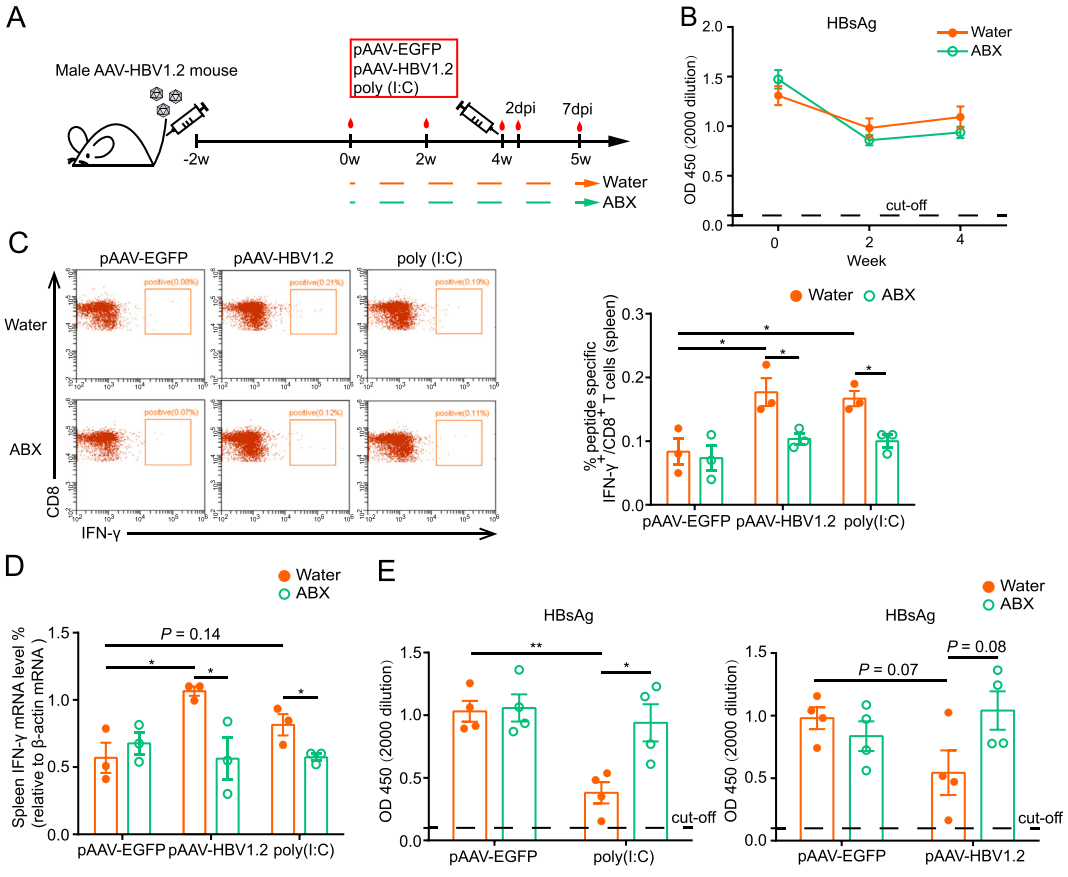

Fig. 6. The effect of antibiotic-induced gut microbiota alteration on HBV replication in male AAV-HBV1.2 mouse model with stimulated HBV immune response. **A** Six-week old male C57BL/6 mice were intravenously injected with 5×10^{10} viral genome recombinant AAV-HBV1.2 to establish persistent HBV replication and then were randomly assigned into water (n = 18) and ABX (n = 18) group. After 4-week antibiotic or water treatment, 6 μg pAAV-EGFP, 6 μg pAAV-HBV1.2 or 20 μg poly(I:C) were injected into mice *via* HDI. The plasmid pAAV-EGFP was negative control. **B** The serum HBsAg level during 4-week antibiotic treatment was determined before HDI (cut-off value = 0.1). **C** Splenocytes were isolated and stimulated with the peptide $HBs_{190–197}$ for flow cytometry to determine HBV specific T cell immune response. The percentages of IFN-γ^+/CD8$^+$ T cells in the spleen were displayed. **D** Splenic IFN-γ mRNA level was analyzed by qPCR assay with mouse *Actb* as the reference gene. The relative level was calculated by the calibrator-normalized Relative Quantification of LightCycler 480 instrument operator's manual. **E** The serum HBsAg level was showed at day 2 after infection of pAAV-EGFP or poly(I:C) in each group. The HBsAg level was showed at day 7 after infection of pAAV-EGFP or pAAV-HBV1.2 in each group. Data are presented as mean ± standard error of mean. Statistical analysis was performed by Student's unpaired two-tailed *t*-test, $^*P < 0.05$, $^{**}P < 0.01$, ns: no significance.

notably impaired. The procedures of antibiotic administration in HDI mouse model were performed firstly, which indicated the suppression of gut bacteria depletion on HBV immune clearance was in accordance with previous studies. To investigate the effect of gut bacteria on HBV replication in AAV-HBV mouse model, six-week-old female mice were injected with recombinant AAV-HBV1.3 and received antibiotic mixtures at 14 wpi. Results showed that long-term antibiotic exposure up to 38 weeks failed to alter HBV replication outcomes. Given that frequent antibiotic exposure hinders gut bacteria maturation and damages host health (Anthony et al., 2022; Lynn et al., 2021), we next administrated 5-week-old female mice with antibiotics for 8 weeks to impede gut microbiota and then persistent HBV replication was established through AAV-HBV1.2 injection. The unchanged HBV replication markers suggested that antibiotic exposure also did not affect HBV replication even though antibiotics were supplemented before AAV-HBV injection. Taken together, gut bacteria alteration caused by antibiotics has no effect on HBV replication in female AAV-HBV mouse model. Due to the reports that male mouse maintained higher levels of HBV antigens than female mouse (Yang et al., 2014; Kosinska et al., 2017), male AAV-HBV mouse model was thereby generated and was exposed to antibiotic mixture during the experiment period. Likewise, gut bacteria amount declined remarkably after antibiotic administration in male AAV-HBV mice. HBV replication levels were not notably altered even though minor increases of serum HBsAg level and liver HBc protein level were observed in antibiotic-treated group. Furthermore, we speculated that antibiotic-induced gut bacteria might affect HBV replication in AAV-HBV mouse model with elicited immune response. Male AAV-HBV1.2 mouse model was generated and antibiotics were supplanted into drinking water to interfere gut bacteria. The HDI procedures of pAAV-HBV1.2 or poly(I:C) were then performed to disrupt immune tolerance in male AAV-HBV1.2 mouse model. The elevated splenic HBV specific T cell response indicated that HBV immune response was obviously activated. Interestingly, antibiotic exposure contributed to the increase of serum HBsAg level in male AAV-HBV mouse model with disrupted immune tolerance.

AAV-HBV1.3 is an experimental model frequently used (Yang et al., 2014; Teng et al., 2021). Initially, when we obtained negative data regarding the effect of antibiotic treatment on HBV replication, we thought one possibility was that previous studies used AAV-HBV1.2 construct (Chou et al., 2015; Wu et al., 2019). Therefore, we switched to AAV-HBV1.2 for further investigation. As we demonstrated in the manuscript, in both AAV-HBV1.3 and AAV-HBV1.2 viral vector transduction mouse models, depletion of gut bacteria by broad-spectrum antibiotic mixtures showed no effect on HBV replication. However, after breaking the immune tolerance by HDI of HBV plasmid or poly(I:C), antibiotic exposure elevated HBsAg levels. Together, these data support that antibiotic-induced gut bacteria depletion has no effect on HBV replication in HBV immune tolerance mouse model. According to published reports and our data, there was no significant difference regarding HBV persistence, cccDNA formation and immune tolerance between AAV-HBV1.2 and AAV-HBV1.3 models.

Gender disparity resulted in different HBV replication and pathogenesis (Tian et al., 2012; Wang et al., 2012). Females tend to develop more intense immune response to virus than males (Fink et al., 2018; Meier et al., 2009). Lower HBV specific T cell immune response explained higher HBV antigens in male HDI mouse model, which indicated the potential effect of immune differences on HBV persistence in male and female mice (Kosinska et al., 2017).

According to our results, immune tolerance HBV replication model can be generated in both 5–6 weeks old (Figs. 2, 5 and 6) and 12–13 weeks old mice (Fig. 4) *via* AAV-HBV transduction while 95% adults are able to mount T cell immune response to resolve the infection (Ganem, 2004). Therefore, despite the superiority of simulating chronic HBV patients at immune tolerant phase, limitations of AAV-HBV mouse model should be noted considering it fails to represent real HBV infection.

Totally, considering different mouse gender, AAV-HBV injection dose and antibiotic exposure time, our results demonstrated that antibiotic-induced gut bacteria depletion failed to affect HBV replication in AAV-HBV mouse model with immune tolerance, suggesting no specific gut microbes could modulate HBV replication in immune tolerance mouse model.

5. Conclusions

In summary, through eliminating gut bacteria with antibiotics, we investigated the effect of gut bacteria on HBV replication in AAV-HBV mouse model with immune tolerance for the first time. These results could serve as reference materials for exploring the effect of gut bacteria on chronic HBV infection in animal models and patients.

Data availability

All the data generated during the current study are included in the manuscript. Fecal 16S rRNA sequencing raw data are available in the NCBI's Sequence Read Archive (SRA) with accession number: PRJNA911436. All data relevant to the study are available upon request from the corresponding author.

Ethics statement

The animal study protocols were approved by the Ethic Committee of Animal Facility, Wuhan University.

Author contributions

Yanan Bu: methodology, investigation, formal analysis, writing-original draft preparation. Kaitao Zhao: methodology, investigation. Zaichao Xu: methodology, investigation. Yingcheng Zheng: investigation. Rong Hua: investigation. Chuanjian Wu: methodology. Yuchen Xia: conceptualization, supervision, project administration, writing-review and editing, funding acquisition. Xiaoming Cheng: conceptualization, project administration.

Conflict of interest

The authors declare that they have no known competing financial interests or personal relationships that could have appeared to influence the work reported in this paper.

Acknowledgements

We thank the staffs at the Research Center for Medicine and Structural Biology of Wuhan University for technical assistance. This research was funded by the National Natural Science Foundation of China (project no. 81971936), Hubei Province's Outstanding Medical Academic Leader Program, Foundation for Innovative Research Groups of the Natural Science Foundation of Hubei (project no. 2020CFA015), the Fundamental Research Funds for the Central Universities (project no. 2042022kf1215 and 2042021gf0013) and Basic and Clinical Medical Research Joint Fund of Zhongnan Hospital, Wuhan University.

Appendix A. Supplementary data

Supplementary data to this article can be found online at https://doi.org/10.1016/j.virs.2023.04.010.

References

Almeida, J.I., Tenreiro, M.F., Martinez-Santamaria, L., Guerrero-Aspizua, S., Gisbert, J.P., Alves, P.M., Serra, M., Baptista, P.M., 2022. Hallmarks of the human intestinal microbiome on liver maturation and function. J. Hepatol. 76, 694–725.
Anthony, W.E., Wang, B., Sukhum, K.V., D'Souza, A.W., Hink, T., Cass, C., Seiler, S., Reske, K.A., Coon, C., Dubberke, E.R., Burnham, C.D., Dantas, G., Kwon, J.H., 2022.

Acute and persistent effects of commonly used antibiotics on the gut microbiome and resistome in healthy adults. Cell Rep. 39, 110649.
Bertoletti, A., Ferrari, C., 2016. Adaptive immunity in HBV infection. J. Hepatol. 64, S71–S83.
Bolyen, E., Rideout, J.R., Dillon, M.R., Bokulich, N.A., Abnet, C.C., AL-Ghalith, G.A., Alexander, H., Alm, E.J., Arumugam, M., Asnicar, F., Bai, Y., Bisanz, J.E., Bittinger, K., Brejnrod, A., Brislawn, C.J., Brown, C.T., Callahan, B.J., Caraballo-Rodriguez, A.M., Chase, J., Cope, E.K., Da Silva, R., Diener, C., Dorrestein, P.C., Douglas, G.M., Durall, D.M., Duvallet, C., Edwardson, C.F., Ernst, M., Estaki, M., Fouquier, J., Gauglitz, J.M., Gibbons, S.M., Gibson, D.L., Gonzalez, A., Gorlick, K., Guo, J., Hillmann, B., Holmes, S., Holste, H., Huttenhower, C., Huttley, G.A., Janssen, S., Jarmusch, A.K., Jiang, L., Kaehler, B.D., Kang, K.B., Keefe, C.R., Keim, P., Kelley, S.T., Knights, D., Koester, I., Kosciolek, T., Kreps, J., Langille, M.G.I., Lee, J., Ley, R., Liu, Y.X., Loftfield, E., Lozupone, C., Maher, M., Marotz, C., Martin, B.D., Mcdonald, D., Mciver, L.J., Melnik, A.V., Metcalf, J.L., Morgan, S.C., Morton, J.T., Naimey, A.T., Navas-Molina, J.A., Nothias, L.F., Orchanian, S.B., Pearson, T., Peoples, S.L., Petras, D., Preuss, M.L., Pruesse, E., Rasmussen, L.B., Rivers, A., Robeson, M.S., 2Nd, Rosenthal, P., Segata, N., Shaffer, M., Shiffer, A., Sinha, R., Song, S.J., Spear, J.R., Swafford, A.D., Thompson, L.R., Torres, P.J., Trinh, P., Tripathi, A., Turnbaugh, P.J., Ul-Hasan, S., Van der Hooft, J.J.J., Vargas, F., Vazquez-Baeza, Y., Vogtmann, E., Von Hippel, M., Walters, W., et al., 2019. Reproducible, interactive, scalable and extensible microbiome data science using QIIME 2. Nat. Biotechnol. 37, 852–857.
Chou, H.H., Chien, W.H., Wu, L.L., Cheng, C.H., Chung, C.H., Horng, J.H., Ni, Y.H., Tseng, H.T., Wu, D., Lu, X., Wang, H.Y., Chen, P.J., Chen, D.S., 2015. Age-related immune clearance of hepatitis B virus infection requires the establishment of gut microbiota. Proc. Natl. Acad. Sci. U. S. A. 112, 2175–2180.
Croswell, A., Amir, E., Teggatz, P., Barman, M., Salzman, N.H., 2009. Prolonged impact of antibiotics on intestinal microbial ecology and susceptibility to enteric Salmonella infection. Infect. Immun. 77, 2741–2753.
Dion, S., Bourgine, M., Godon, O., Levillayer, F., Michel, M.L., 2013. Adeno-associated virus-mediated gene transfer leads to persistent hepatitis B virus replication in mice expressing HLA-A2 and HLA-DR1 molecules. J. Virol. 87, 5554–5563.
Drummond, R.A., Desai, J.V., Ricotta, E.E., Swamydas, M., Deming, C., Conlan, S., Quinones, M., Matei-Rascu, V., Sherif, L., Lecky, D., Lee, C.R., Green, N.M., Collins, N., Zelazny, A.M., Prevots, D.R., Bending, D., Withers, D., Belkaid, Y., Segre, J.A., Lionakis, M.S., 2022. Long-term antibiotic exposure promotes mortality after systemic fungal infection by driving lymphocyte dysfunction and systemic escape of commensal bacteria. Cell Host Microbe 30, 1020–1033.e6.
Du, Y., Broering, R., Li, X., Zhang, X., Liu, J., Yang, D., Lu, M., 2021. In vivo mouse models for hepatitis B virus infection and their application. Front. Immunol. 12, 766534.
Durack, J., Lynch, S.V., 2019. The gut microbiome: relationships with disease and opportunities for therapy. J. Exp. Med. 216, 20–40.
Erttmann, S.F., Swacha, P., Aung, K.M., Brindefalk, B., Jiang, H., Hartlova, A., Uhlin, B.E., Wai, S.N., Gekara, N.O., 2022. The gut microbiota prime systemic antiviral immunity via the cGAS-STING-IFN-I axis. Immunity 55, 847–861.e10.
Fink, A.L., Engle, K., Ursin, R.L., Tang, W.Y., Klein, S.L., 2018. Biological sex affects vaccine efficacy and protection against influenza in mice. Proc. Natl. Acad. Sci. U. S. A. 115, 12477–12482.
Fox, J.G., Feng, Y., Theve, E.J., Raczynski, A.R., Fiala, J.L., Doernte, A.L., Williams, M., Mcfaline, J.L., Essigmann, J.M., Schauer, D.B., Tannenbaum, S.R., Dedon, P.C., Weinman, S.A., Lemon, S.M., Fry, R.C., Rogers, A.B., 2010. Gut microbes define liver cancer risk in mice exposed to chemical and viral transgenic hepatocarcinogens. Gut 59, 88–97.
Ganem, D., 2004. Hepatitis B virus infection - Natural history and clinical consequences (vol 350, pg 1118, 2004). N. Engl. J. Med. 351, 1268, 1268.
Guo, W., Zhou, X., Li, X., Zhu, Q., Peng, J., Zhu, B., Zheng, X., Lu, Y., Yang, D., Wang, B., Wang, J., 2021. Depletion of gut microbiota impairs gut barrier function and antiviral immune defense in the liver. Front. Immunol. 12, 636803.
Huang, H., Ren, Z., Gao, X., Hu, X., Zhou, Y., Jiang, J., Lu, H., Yin, S., Ji, J., Zhou, L., Zheng, S., 2020. Integrated analysis of microbiome and host transcriptome reveals correlations between gut microbiota and clinical outcomes in HBV-related hepatocellular carcinoma. Genome Med. 12, 102.
Huang, L.R., Wu, H.L., Chen, P.J., Chen, D.S., 2006. An immunocompetent mouse model for the tolerance of human chronic hepatitis B virus infection. Proc. Natl. Acad. Sci. U. S. A. 103, 17862–17867.
Joo, E.J., Cheong, H.S., Kwon, M.J., Sohn, W., Kim, H.N., Cho, Y.K., 2021. Relationship between gut microbiome diversity and hepatitis B viral load in patients with chronic hepatitis B. Gut Pathog. 13, 65.
Kosinska, A.D., Pishraft-Sabet, L., Wu, W., Fang, Z., Lenart, M., Chen, J., Dietze, K.K., Wang, C., Kemper, T., Lin, Y., Yeh, S.H., Liu, J., Dittmer, U., Yuan, Z., Roggendorf, M., Lu, M., 2017. Low hepatitis B virus-specific T-cell response in males correlates with high regulatory T-cell numbers in murine models. Hepatology 66, 69–83.
Lee, H.M., Banini, B.A., 2019. Updates on chronic HBV: current challenges and future goals. Curr. Treat. Options Gastroenterol. 17, 271–291.
Lucifora, J., Salvetti, A., Marniquet, X., Mailly, L., Testoni, B., Fusil, F., Inchauspe, A., Michelet, M., Michel, M.L., Levrero, M., Cortez, P., Baumert, T.F., Cosset, F.L., Challier, C., Zoulim, F., Durantel, D., 2017. Detection of the hepatitis B virus (HBV) covalently-closed-circular DNA (cccDNA) in mice transduced with a recombinant AAV-HBV vector. Antivir. Res. 145, 14–19.
Lynn, M.A., Eden, G., Ryan, F.J., Bensalem, J., Wang, X., Blake, S.J., Choo, J.M., Chern, Y.T., Sribnaia, A., James, J., Benson, S.C., Sandeman, L., Xie, J., Hassiotis, S., Sun, E.W., Martin, A.M., Keller, M.D., Keating, D.J., Sargeant, T.J., Proud, C.G., Wesselingh, S.L., Rogers, G.B., Lynn, D.J., 2021. The composition of the gut microbiota following early-life antibiotic exposure affects host health and longevity in later life. Cell Rep. 36, 109564.
Meier, A., Chang, J.J., Chan, E.S., Pollard, R.B., Sidhu, H.K., Kulkarni, S., Wen, T.F., Lindsay, R.J., Orellana, L., Mildvan, D., Bazner, S., Streeck, H., Alter, G., Lifson, J.D., Carrington, M., Bosch, R.J., Robbins, G.K., Altfeld, M., 2009. Sex differences in the Toll-like receptor-mediated response of plasmacytoid dendritic cells to HIV-1. Nat. Med. 15, 955–959.
Morgun, A., Dzutsev, A., Dong, X., Greer, R.L., Sexton, D.J., Ravel, J., Schuster, M., Hsiao, W., Matzinger, P., Shulzhenko, N., 2015. Uncovering effects of antibiotics on the host and microbiota using transkingdom gene networks. Gut 64, 1732–1743.
Ren, Y.D., Ye, Z.S., Yang, L.Z., Jin, L.X., Wei, W.J., Deng, Y.Y., Chen, X.X., Xiao, C.X., Yu, X.F., Xu, H.Z., Xu, L.Z., Tang, Y.N., Zhou, F., Wang, X.L., Chen, M.Y., Chen, L.G., Hong, M.Z., Ren, J.L., Pan, J.S., 2017. Fecal microbiota transplantation induces hepatitis B virus e-antigen (HBeAg) clearance in patients with positive HBeAg after long-term antiviral therapy. Hepatology 65, 1765–1768.
Teng, Y., Xu, Z., Zhao, K., Zhong, Y., Wang, J., Zhao, L., Zheng, Z., Hou, W., Zhu, C., Chen, X., Protzer, U., Li, Y., Xia, Y., 2021. Novel function of SART1 in HNF4alpha transcriptional regulation contributes to its antiviral role during HBV infection. J. Hepatol. 75, 1072–1082.
Tian, Y., Kuo, C.F., Chen, W.L., Ou, J.H., 2012. Enhancement of hepatitis B virus replication by androgen and its receptor in mice. J. Virol. 86, 1904–1910.
Tripathi, A., Debelius, J., Brenner, D.A., Karin, M., Loomba, R., Schnabl, B., Knight, R., 2018. The gut-liver axis and the intersection with the microbiome. Nat. Rev. Gastroenterol. Hepatol. 15, 397–411.
Wang, J., Zhou, X., Li, X., Guo, W., Zhu, Q., Zhu, B., Lu, Y., Zheng, X., Yang, D., Wang, B., 2022. Fecal microbiota transplantation alters the outcome of hepatitis B virus infection in mice. Front. Cell. Infect. Microbiol. 12, 844132.
Wang, S.H., Yeh, S.H., Lin, W.H., Yeh, K.H., Yuan, Q., Xia, N.S., Chen, D.S., Chen, P.J., 2012. Estrogen receptor alpha represses transcription of HBV genes via interaction with hepatocyte nuclear factor 4alpha. Gastroenterology 142, 989–998.e4.
Wang, X., Zhu, J., Zhang, Y., Li, Y., Ma, T., Li, Q., Xu, J., Xu, L., 2018. The doses of plasmid backbone plays a major role in determining the HBV clearance in hydrodynamic injection mouse model. Virol. J. 15, 89.
Wargo, J.A., 2020. Modulating gut microbes. Science 369, 1302–1303.
Wu, T., Li, F., Chen, Y., Wei, H., Tian, Z., Sun, C., Sun, R., 2019. CD4(+) T cells play a critical role in microbiota-maintained anti-HBV immunity in a mouse model. Front. Immunol. 10, 927.
Xia, Y., Cheng, X., Blossey, C.K., Wisskirchen, K., Esser, K., Protzer, U., 2017. Secreted interferon-inducible factors restrict hepatitis B and C virus entry in vitro. J Immunol Res 2017, 4828936.
Xia, Y., Liang, T.J., 2019. Development of direct-acting antiviral and host-targeting agents for treatment of hepatitis B virus infection. Gastroenterology 156, 311–324.
Xu, Z., Zhao, L., Zhong, Y., Zhu, C., Zhao, K., Teng, Y., Cheng, X., Chen, Q., Xia, Y., 2022. A novel mouse model harboring hepatitis B virus covalently closed circular DNA. Cell Mol Gastroenterol Hepatol 13, 1001–1017.
Yan, H., Zhong, G.C., Xu, G.W., He, W.H., Jing, Z.Y., Gao, Z.C., Huang, Y., Qi, Y.H., Peng, B., Wang, H.M., Fu, L.R., Song, M., Chen, P., Gao, W.Q., Ren, B.J., Sun, Y.Y., Cai, T., Feng, X.F., Sui, J.H., Li, W.H., 2012. Sodium taurocholate cotransporting polypeptide is a functional receptor for human hepatitis B and D virus. Elife 1, e00049.
Yang, D., Liu, L., Zhu, D., Peng, H., Su, L., Fu, Y.X., Zhang, L., 2014. A mouse model for HBV immunotolerance and immunotherapy. Cell. Mol. Immunol. 11, 71–78.
Yang, X.A., Lv, F., Wang, R., Chang, Y., Zhao, Y., Cui, X., Li, H., Yang, S., Li, S., Zhao, X., Mo, Z., Yang, F., 2020. Potential role of intestinal microflora in disease progression among patients with different stages of Hepatitis B. Gut Pathog. 12, 50.
Zarrinpar, A., Chaix, A., Xu, Z.Z., Chang, M.W., Marotz, C.A., Saghatelian, A., Knight, R., Panda, S., 2018. Antibiotic-induced microbiome depletion alters metabolic homeostasis by affecting gut signaling and colonic metabolism. Nat. Commun. 9, 2872.